

Supplementary information for

Peptide Metal-Organic Frameworks under pressure: flexible linkers for cooperative compression

José Navarro-Sánchez, Ismael Mullor-Ruiz, Catalin Popescu, David Santamaría-Pérez, Alfredo Segura, Daniel Errandonea, Javier González-Platas and Carlos Martí-Gastaldo

Table of Contents

SI1. General considerations: starting materials and characterization	2
Materials and reagents	2
Physical and chemical characterization.....	2
SI2. Synthesis and characterization of Zn(GlyTyr)₂.....	3
Figure SI1. Optical microscope and of as-made crystals of Zn(Gly-Tyr) ₂	3
Figure SI2. Scanning Electron Microscopy (SEM) images.....	3
Figure SI3. FT-IR of Zn(Gly-Tyr) ₂	3
Figure SI4. Thermogravimetric analysis of Zn(Gly-Tyr) ₂	4
Figure SI6. Chiral dichroism (CD) UV-Vis spectrum of Gly-Tyr (blue) and Zn(Gly-Tyr)2 (green).....	5
SI3. X-Ray diffraction and structure of Zn(GlyTyr)₂.....	6
Table SI1. Crystal data and structure refinement for Zn(GlyTyr) ₂ at environmental pressure.....	6
Figure SI7. Ortep representation (50% probability) of the asymmetric unit of Zn(GlyTyr) ₂	7
Table SI2. Hydrogen bonds for Zn(GlyTyr) ₂	7
Figure SI8. Structure of (a) Zn(GlyAla) ₂ , (b) Zn(GlySer) ₂ , and (c) Zn(GlyThr) ₂	7
SI4. Powder High-Pressure X-Ray diffraction and effect of Pressure Transmitting Media over structural response	9
Figure SI9. High-pressure powder diffraction data in methanol.	9
Figure SI10. High-pressure powder diffraction data in ethanol.	10
Figure SI11. High-pressure powder diffraction data in dimethylformamide.....	11
Figure SI12. High-pressure powder diffraction data in Fluorinert (FC-70).....	12
Figure SI13. Evolution of the unit cell parameters with pressure.	13
SI5. Single-crystal High-Pressure X-Ray diffraction.....	14
Single-crystal HP-XRD experiments.....	14
Figure SI14. (<i>left</i>) Variation of the unit cell volume of Zn(GlyTyr) ₂ with increasing pressure. (<i>right</i>) Plot of normalized pressure vs data strain.	14
Table SI3. BM3 EoS parameters for single crystal Zn(GlyTyr) ₂	14
Figure SI15. Comparison of the variation of the volume, cell parameters and beta angle.	15
Table SI4. Crystal data and HP structure refinement for Zn(GlyTyr) ₂ between 0.51 and 3.95 GPa.	15
Figure SI16. Comparison of the variation of the cell changes normalized to their value at ambient pressure for the crystallographic directions [-101], [010] and [101].	17
Figure SI17. Changes in the distance of the π-π interactions between 0-3.95 GPa defined as the distance between the centroid of neighbouring aromatic rings in the sidechain of Tyr.	17
Table SI5. Summary of the evolution of the parameters used for analysing the structural changes in Zn(GlyTyr) ₂	18
SI6. References	20

SI1. General considerations: starting materials and characterization

Materials and reagents

All reagents and solvents used were of commercially available grade and were used without any additional purification. The dipeptide H-Gly-Tyr-OH and the metal salt Zn(NO₃)₂.6H₂O was purchased from Sigma®. Methanol and toluene were supplied by Scharlau. Ultrapure water was obtained from a Nanopure II (Sybron) system.

Physical and chemical characterization

- Carbon, nitrogen and hydrogen contents were determined by microanalytical procedures using a LECO CHNS.
- Infrared spectra were recorded in an Agilent Cary 630 FTIR Spectrometer directly with KBr pellets.
- Thermogravimetric analysis was carried out with a Mettler Toledo TGA/SDTA 851e apparatus between 25 and 800 °C under ambient conditions (10 °C·min⁻¹ scan rate and an air flow of 30 mL·min⁻¹)
- Powder XRD patterns were collected in a PANalytical X'Pert PRO diffractometer using copper radiation (Cu K α = 1.5418 Å) with an X'Celerator detector, operating at 40 mA and 45 kV. Profiles were collected in the 2° < 2θ < 40° range with a step size of 0.017°.
- Single-crystal XRD data at room pressure was collected in a Rigaku SuperNOVA diffractometer equipped with an ATLAS detector (CCD) and Cu radiation micro-source (Cu K α = 1.54184 Å).
- Angle dispersive powder HP-XRD were performed at MSPD beamline of Alba synchrotron light source using a monochromatic beam (λ =0.4246 Å). The 2D patterns were collected using a Rayonix SX165 CCD detector located at 350 mm away from the sample and then integrated using FIT2D. The typical acquisition time was 20 s.
- Single-crystal HP-XRD was performed at MSPD beamline of Alba synchrotron light source with a wavelength of λ =0.3185 Å focused down to 20x20 μm² (FWHM). The diffraction images were collected by 0.2° ω scanning using a Rayonix SX165 CCD detector placed 170 mm away from the sample.
- NIKON Eclipse LV-100 Optical microscope equiped with a digital camera: Nikon, D7000 AF-S DX NiKKOR 18-105mm f/3.5-5.6G ED VR was used for taking pictures of the crystals.
- Chiral dichroism (CD) UV-Vis spectrum was collected with a spectropolarimeter Jasco J-810.

SI2. Synthesis and characterization of Zn(GlyTyr)₂

Synthesis of Zn(GlyTyr)₂. 47.6 mg of Gly-Tyr (0.2 mmol) are dissolved in 7.6 mL of a Zn(NO₃)₂.6H₂O 0.13M methanolic solution in a 12 mL scintillation vial. The mixture is hand shaken to render a colourless solution followed by addition of 4 mL of toluene. The mixture is mechanically stirred for 15 minutes and then transferred to an oven and heated at 85°C for two minutes. This results on the formation of colourless crystals that are isolated by filtration, washed thoroughly with methanol and left to stand at room temperature for drying. This protocol was repeated 5 times to produce a total of 270 mg (30% yield calculated for zinc).

Analysis. calc. for Zn(C₁₅H₂₀O₄N₂) (Mw: 357.71) Calc. C: 48.95 H: 4.85 N: 10.38. Found: C:47.98 H:5.01 N: 10.27

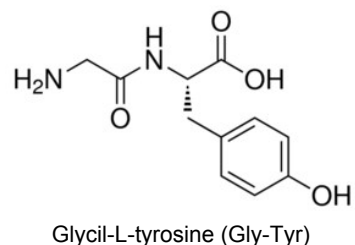


Figure SI1. Optical microscope and of as-made crystals of Zn(Gly-Tyr)₂.

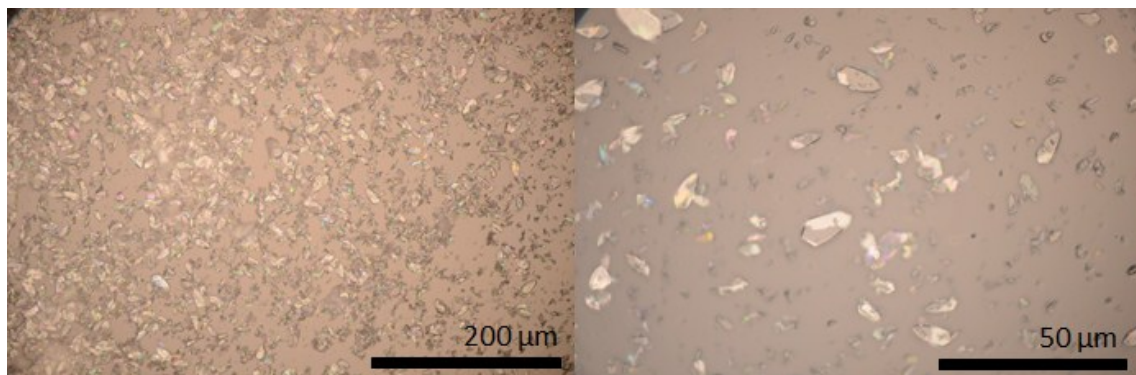


Figure SI2. Scanning Electron Microscopy (SEM) images. Particle morphologies and dimensions were studied with a Hitachi S-4800 scanning electron microscope at an accelerating voltage of 20 keV, over metalized samples with a mixture of gold and palladium during 30 s.

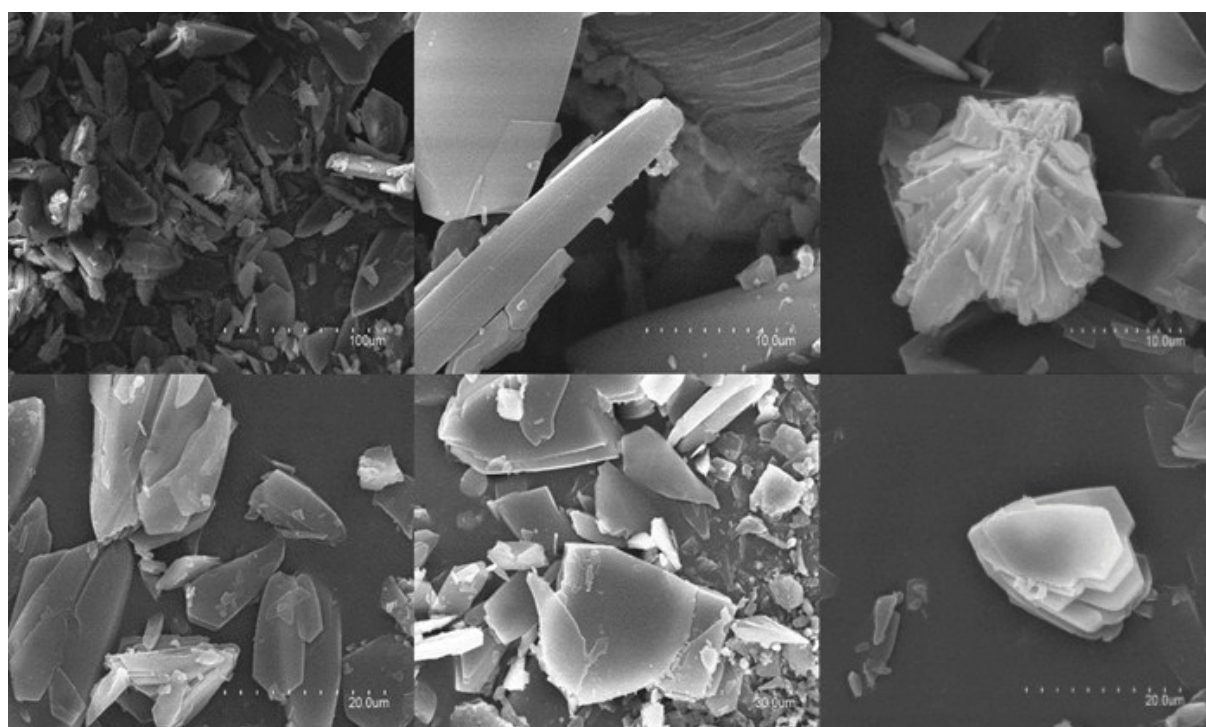
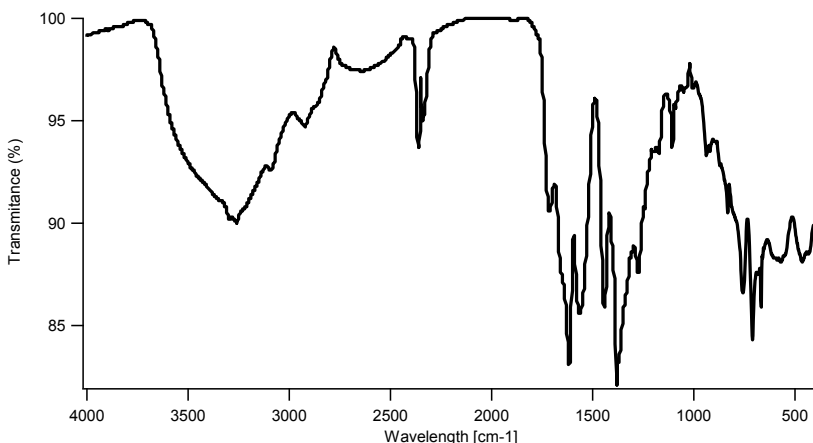
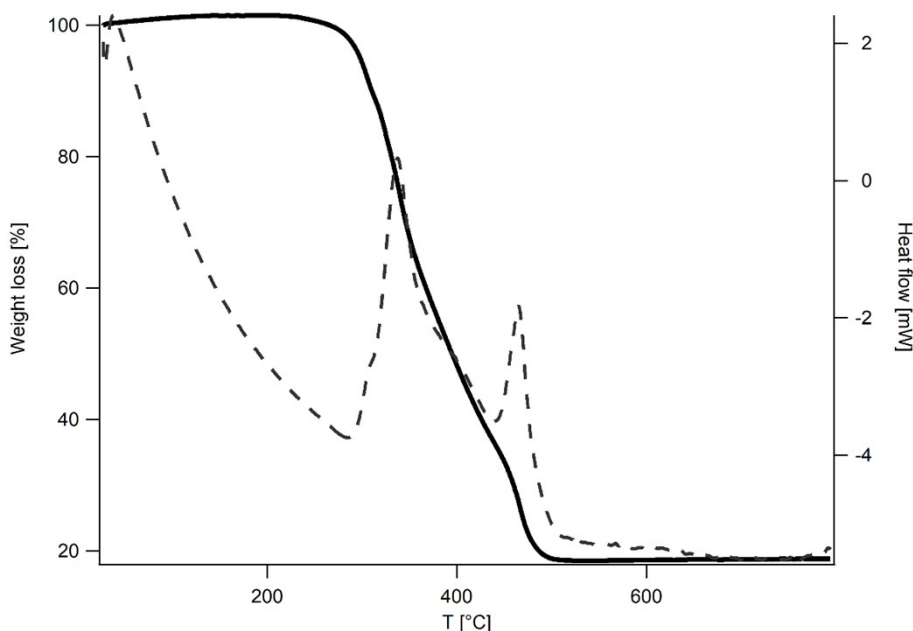


Figure SI3. FT-IR of Zn(Gly-Tyr)₂ collected in a FT-IR Nicolet 5700 spectrometer in the 4000–400 cm⁻¹ range from ground crystals diluted in a KBr pellet.



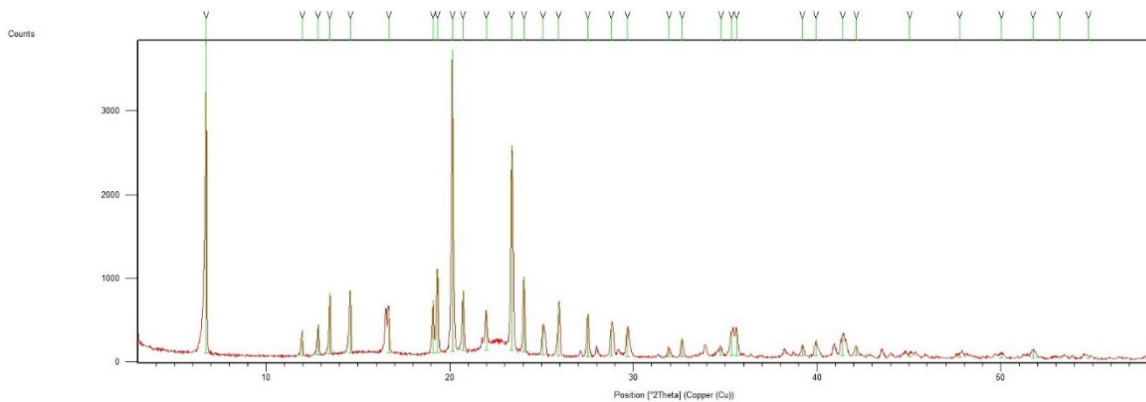
(KBr, [cm⁻¹]): 300 (m), 610 (m), 1200 (m), 1400 (m), 1600 (m), 2400 (w), 2900 (w), 2450 (sr, br), 3700 (w).

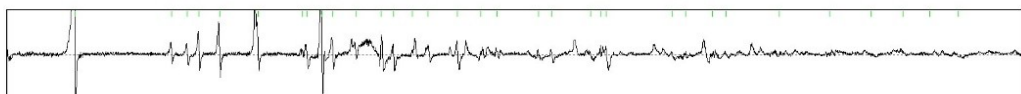
Figure S14. Thermogravimetric analysis of Zn(Gly-Tyr)₂ between 25 and 800 °C under a 5 °C·min⁻¹ scan rate and an air flow of 30 mL·min⁻¹ by using a Mettler Toledo TGA/SDTA 851.



There is no weight loss at low temperature that confirms the dense structure of Zn(GlyTyr)₂.

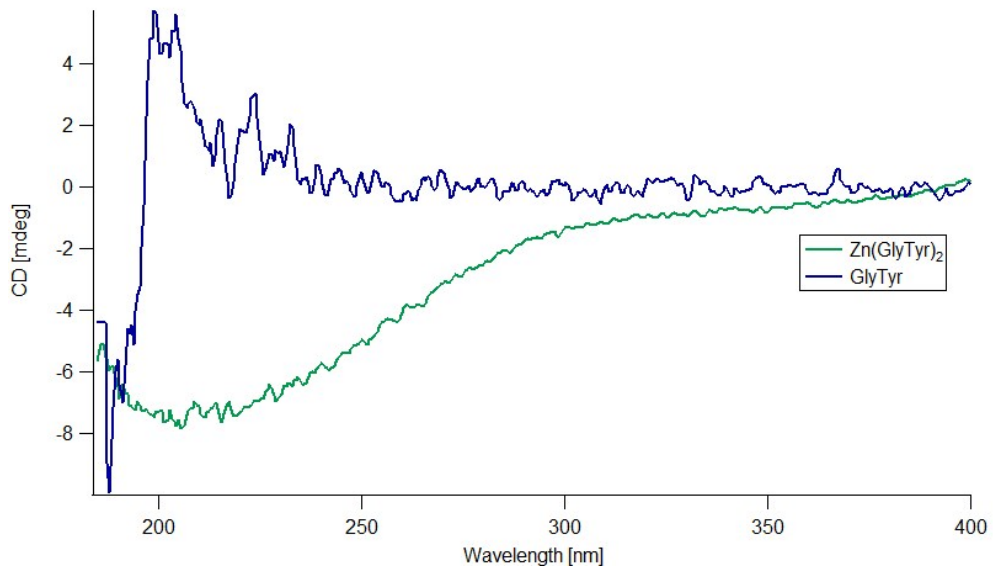
Figure S15. Experimental PXRD (red line), calculated (blue line), difference plot [(Iobs-Icalcd)] (black line, bottom panel) and Bragg positions (green dashed line) for the unit cell refinement of experimental diffraction data of Zn(Gly-Tyr)₂ collected at room temperature by using experimental single-crystal data as starting parameters.¹ PXRD patterns were collected in a PANalytical X'Pert PRO diffractometer using copper radiation ($\text{Cu K}\alpha = 1.5418 \text{ \AA}$) with an X'Celerator detector, operating at 40 mA and 45 kV. Profiles were collected in the $2^\circ < 2\theta < 60^\circ$ range with a step size of 0.017°.





Monoclinic, I 2; $a = 7.4716(5)$, $b = 5.4271(3)$, $c = 26.6069(14) \text{ \AA}$; $V = 1068.21 \text{ \AA}^3$. $\chi^2 = 1.529\text{E-}06$. Snyder's FOM = 4.7898.

Figure SI6. Chiral dichroism (CD) UV-Vis spectrum of Gly-Tyr (blue) and Zn(Gly-Tyr)₂ (green). Solution used for the measurements was prepared by diluting ground crystals of the MOF in ultrapure water. Spectra was collected with a spectropolarimeter Jasco J-810 and recorded at a temperature of 25°C. Ellipticity values were recorded every 0.5 nm at a wavelength scanning speed of 100 nm/min. The response time was set to 1 s and the bandwidth was set to 1 nm. The final spectrum represented the accumulated average of ten consecutive scans with baseline correction. As the free dipeptide gives a shift in the area of the peptidic bond (displays a negative Cotton effect in the UV region linked to the presence of enantiopure dipeptide), the other one has a negative adsorption due to Zn (II) complexation.



SI3. X-Ray diffraction and structure of Zn(GlyTyr)₂

X-ray diffraction (XRD) measurement was collected at room temperature by using a Rigaku SuperNOVA diffractometer equipped with an EOS detector (CCD) and Mo radiation micro-source ($\lambda=0.71073\text{\AA}$) and CrysAlisPro software¹ was used to process the data. The structure of the compound at rt was determined by a dual-space algorithm using the SHELXT program,² and refinement was performed using SHELXL program³ against F^2 by full-matrix least-squares refinement. All non-hydrogen atoms were refined anisotropically and hydrogen atoms were included in the model at calculated positions, and refined with a rigid model with their U_{iso} value to 1.2 U_{eq} of their parent atoms. The PLATON program⁴ has been used for geometric calculations.

Crystallographic data for the structures reported in this contribution have been deposited with the Cambridge Crystallographic Data Centre as supplementary publication. Copies of the data can be obtained free of charge on application to the CCDC, Cambridge, U.K. (<http://www.ccdc.cam.ac.uk/>).

Table SI1. Crystal data and structure refinement for Zn(GlyTyr)₂ at environmental pressure.

Identification code	1588160
Empirical formula	C ₂₂ H ₂₆ N ₄ O ₈ Zn
M	539.84
Cryst. Syst.	Monoclinic
Space group	I2
a, Å	7.4908 (2)
b, Å	5.4877 (2)
c, Å	26.5634 (10)
α , °	90
β , °	97.740 (3)
γ , °	90
V, Å ³	1082.00 (6)
Z	2
D _o /g cm ⁻³	1.657
F(000)	560
μ (Mo K α), mm ⁻¹	2.109
Reflections (collected/unique, (Rint))	4430/2206/0.019
Data/restrains/paramet ers	2206/1/160
R1, wR [F ² >2 σ (F ²)]	0.025/0.065
Goodness-of-fit on F ²	1.048
Largest diff. peak and hole (e Å ⁻³)	0.27/-0.21
Flack parameter	0.014(13)

Refinement model description: number of restraints – 0; number of constraints – 0.

Figure SI7. Ortep representation (50% probability) of the asymmetric unit of Zn(GlyTyr)₂.

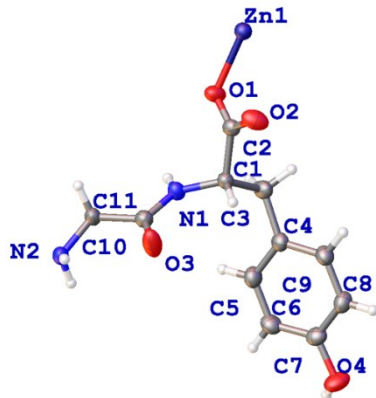
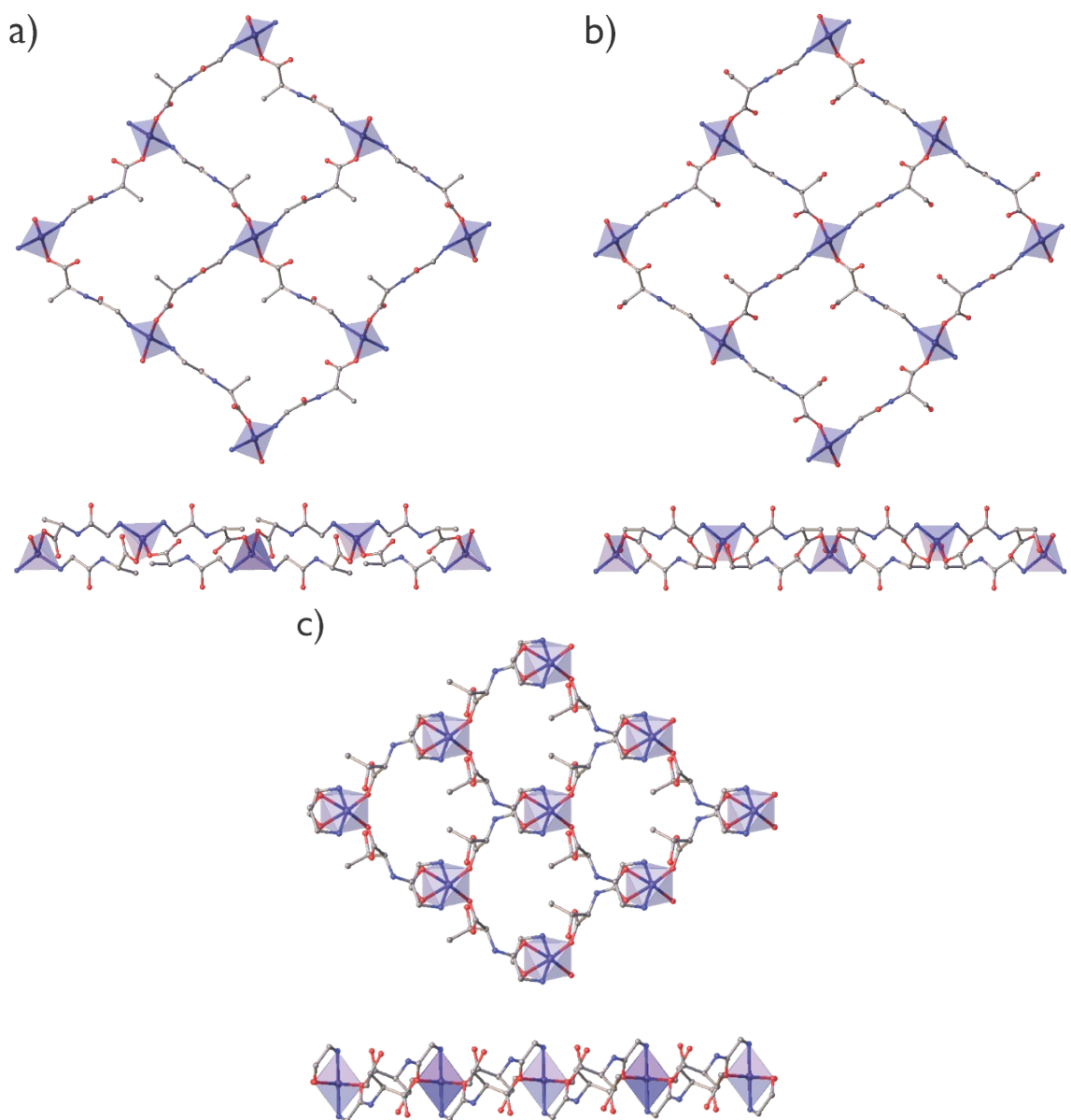


Table SI2. Hydrogen bonds for Zn(GlyTyr)₂.

D	H	A	d(D-H)/Å	d(H-A)/Å	d(D-A)/Å	D-H-A/°
N1	H1	O2(i)	0.86	1.98	2.831(4)	169
N2	H2B	O4(ii)	0.89	2.23	2.987(3)	143
O4	H4	O3(ii)	0.82	1.89	2.643(4)	152
N2	H2A	O3	0.89	2.46	2.789(4)	102

(i) x,1+y,z (ii) 3/2-x,1/2+y,3/2-z

Figure SI8. Structure of (a) Zn(GlyAla)₂,⁵ (b) Zn(GlySer)₂,⁶ and (c) Zn(GlyThr)₂.⁷ Neutral layers are represented along parallel (top) and perpendicular directions (bottom).



SI4. Powder High-Pressure X-Ray diffraction and effect of Pressure Transmitting Media over structural response

Five series of synchrotron-based powder XRD experiments under compression were performed using different pressure media: Fluorinert FC-70 (Figure SI8), methanol (Figure SI9), ethanol (Figure SI10), dimethylformamide (Figure SI11) and methanol and water 3:1 in volume (Figure 2 in the text). The maximum pressure reached was 10 GPa, but due to peak broadening and partial amorphization we only show the data below 6 GPa. Angle-dispersive XRD experiments were carried out using diamond-anvil cells (DAC) with diamond culets of 500 and 700 μm . The pressure chamber was a 200-300 μm hole drilled on a 40- μm pre-indented Inconel gasket. Pressure was determined by using ruby fluorescence.⁸ Particular attention was paid to avoid sample bridging between the diamond anvils.⁹ Experiments were performed at the materials science and powder diffraction (MSPD) beamline of the ALBA synchrotron.¹⁰ A monochromatic beam ($\lambda = 0.4246 \text{ \AA}$) focused to a beam size down to 20 $\mu\text{m} \times 20 \mu\text{m}$ (FWHM) using Kirkpatrick-Baez mirrors. The two-dimensional XRD patterns were collected using a Rayonix SX165 CCD detector and integrated with FIT2D¹¹, while structural analyses were performed with GSAS.¹²

Figure SI9. High-pressure powder diffraction data in methanol.

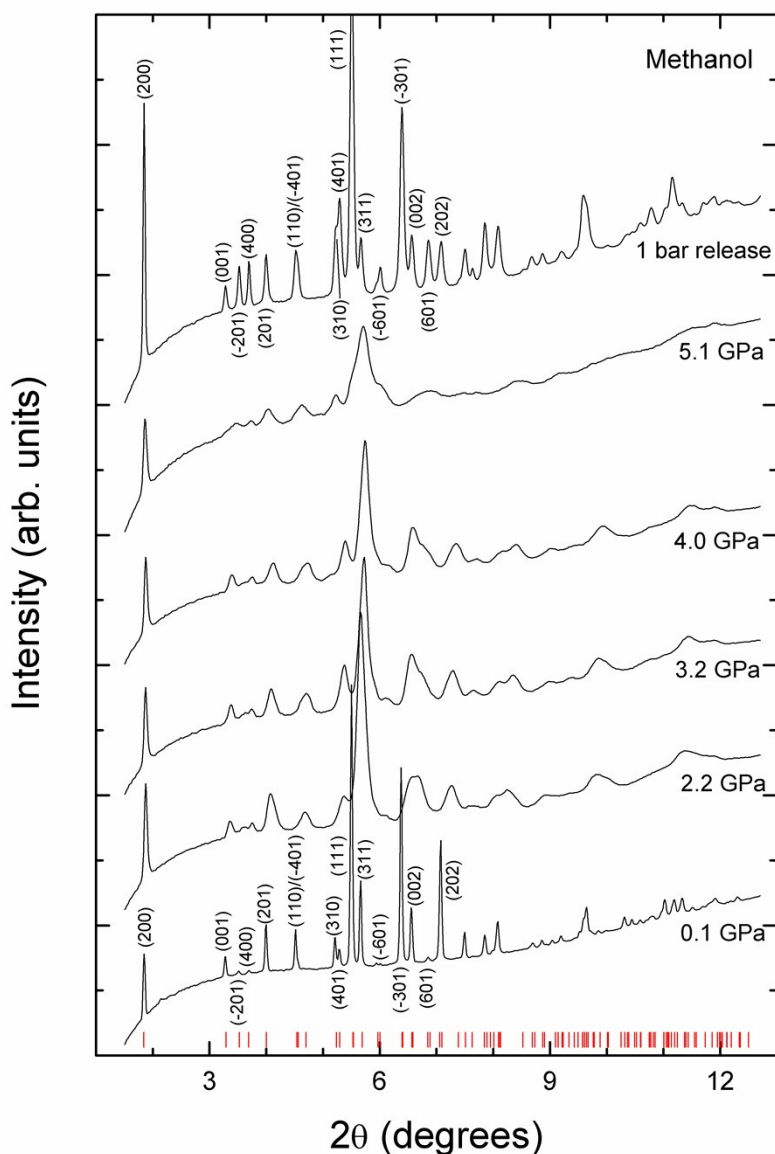


Figure S110. High-pressure powder diffraction data in ethanol.

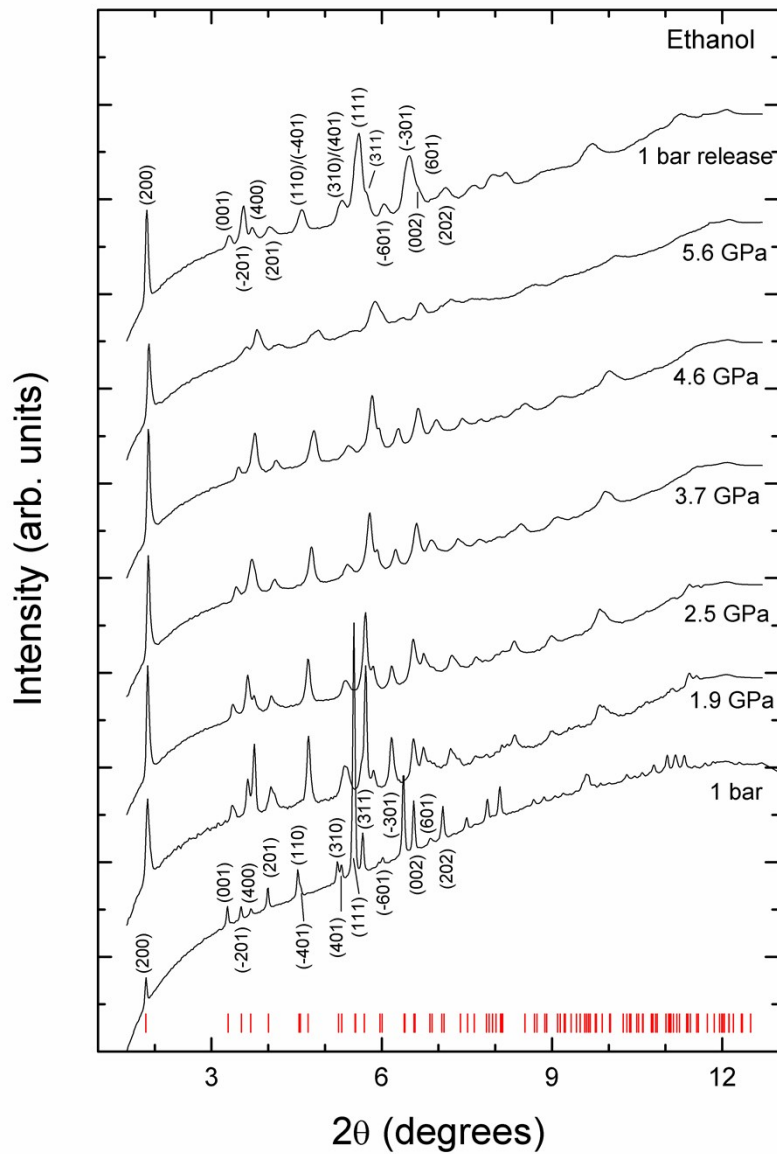


Figure S11. High-pressure powder diffraction data in dimethylformamide. The two new diffraction lines observed at low angles correspond to Bragg peaks of DMF.

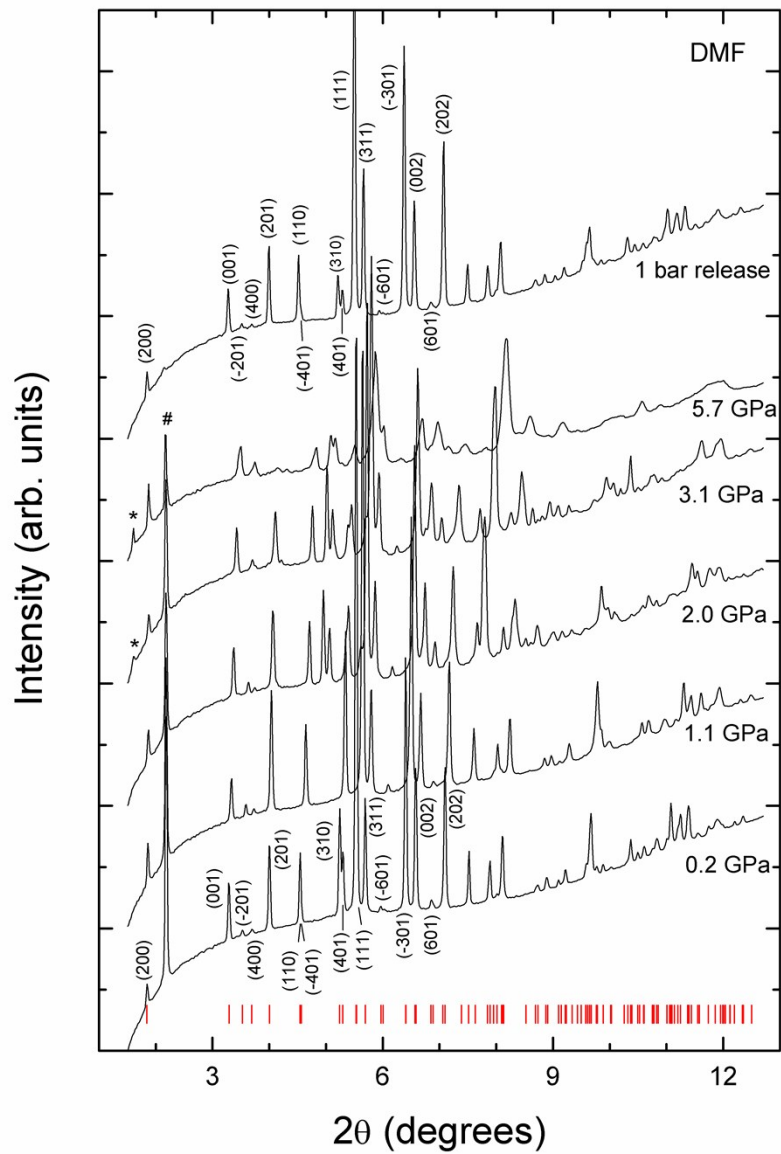


Figure S112. High-pressure powder diffraction data in Fluorinert (FC-70).

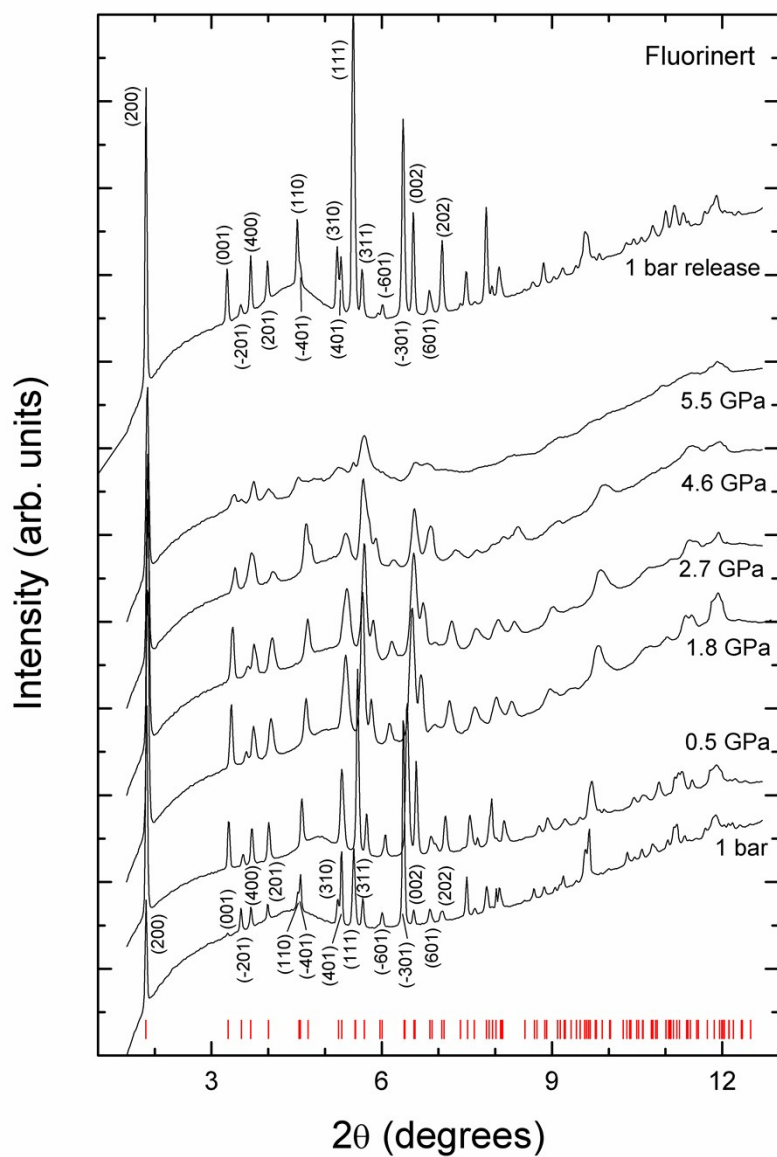
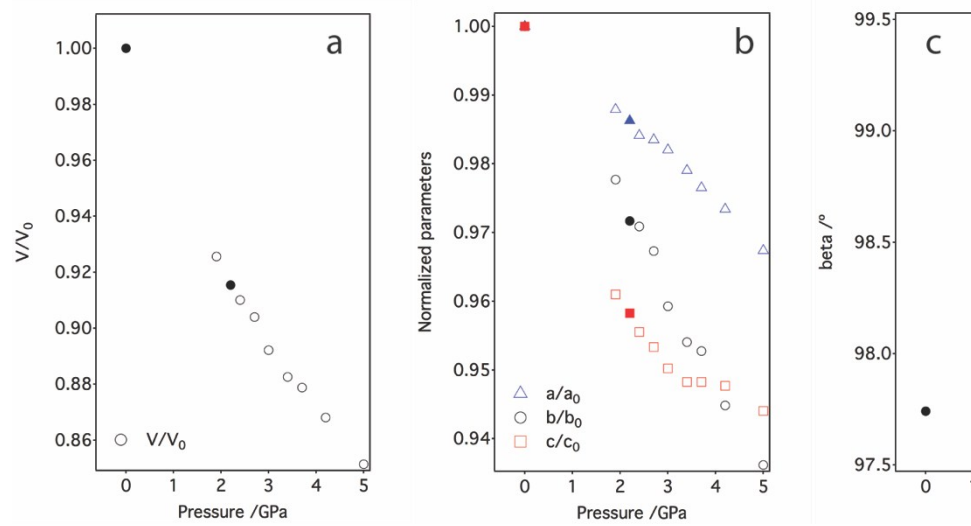


Figure SI13. Evolution of the unit cell parameters with pressure for the HP-PXRD experiments performed in MeOH:water (25:75). From left to right changes in: volume, cell axis and beta values. Solid symbols stand for the first set of experiments upon increasing pressure. Empty symbols were obtained after releasing pressure. The coincidence between increasing and decreasing pressures suggest that the compression of the material proceeds reversibly.



SI5. Single-crystal High-Pressure X-Ray diffraction

Single-crystal HP-XRD experiments. For high-pressure measurements, we have used a Diacell Bragg-Mini diamond anvil cell (DAC) from Almax-EasyLab, with an opening angle of 85° and anvil culets of 500 μm diameter, fitted with a stainless gasket containing a hole of 200 μm diameter and 50 μm depth. A mixture of methanol-ethanol-water (16:3:1 in volume) was used as pressure-transmitting medium, which remains hydrostatic in the range of pressure used in our experiments^{13,14} in order to minimize deviatoric stresses which can cause incorrect values for bulk modulus.¹⁵ The sample was placed on one of the diamonds anvils (diffraction side) together with a small ruby sphere as pressure sensor. The single-crystal XRD experiment was performed at MSPD beamline with a wavelength of $\lambda = 0.3185 \text{ \AA}$ determined from the La absorption K-edge (38.92 keV). The sample-detector distance (170 mm) and the beam centre position were calibrated using the FIT2D software from LaB₆ diffraction data measured at exactly the same conditions as the sample. The exploration of the reciprocal space was performed by rotation the DAC around the Φ axis and performing small scans ($\Delta\omega=0.2^\circ$, time/frame=0.5 s) covering an ω range between -30° and +30°. The structure was refined, for each pressure, using previous results as starting point, on F^2 by full-matrix least-squares refinement using the SHELXL program. Due to limitations of the opening angle of our DAC it is only possible to collect about 20-30% of the total reflections present in a full dataset at ambient conditions. In this situation, structure refinements were performed with isotropic displacement parameters for all atoms except for zinc atom that was refined with anisotropic displacement parameters whenever it did not become non-positive definite. Hydrogen atoms were included in the final procedure in the same way as for ambient conditions. No restraints were used during this process.

Crystallographic data for the structures reported in this contribution have been deposited with the Cambridge Crystallographic Data Centre as supplementary publication 1588161-1588166. Copies of the data can be obtained free of charge on application to the CCDC, Cambridge, U.K. (<http://www.ccdc.cam.ac.uk/>).

Figure SI14. (left) Variation of the unit cell volume of Zn(GlyTyr)₂ with increasing pressure. Error bars are smaller than their respective size symbols. The curve was fit to a third-order Birch-Murnaghan function. Dashed line corresponds to the EoS model fit. (right) Plot of normalized pressure vs data strain (Ff) confirms that model used is consistent with the experimental data.

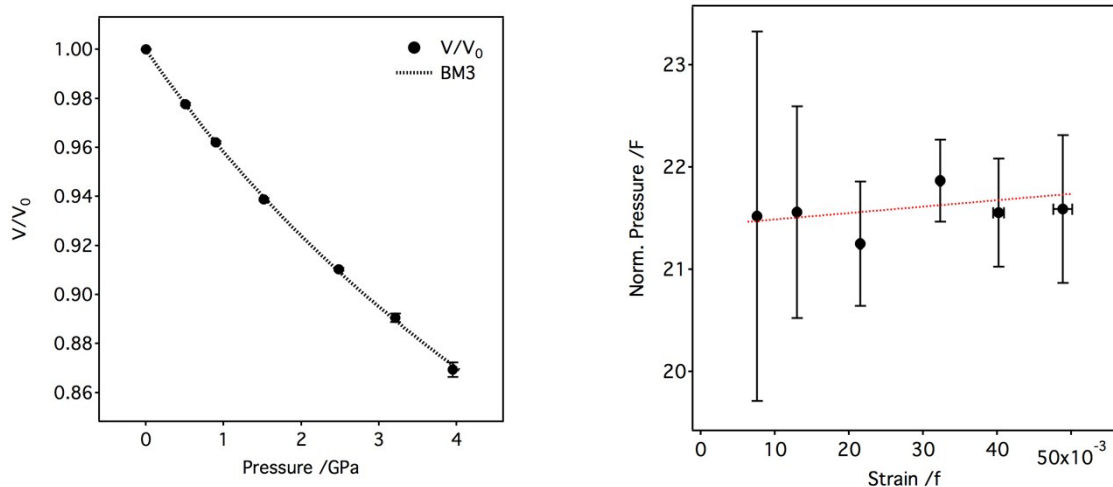


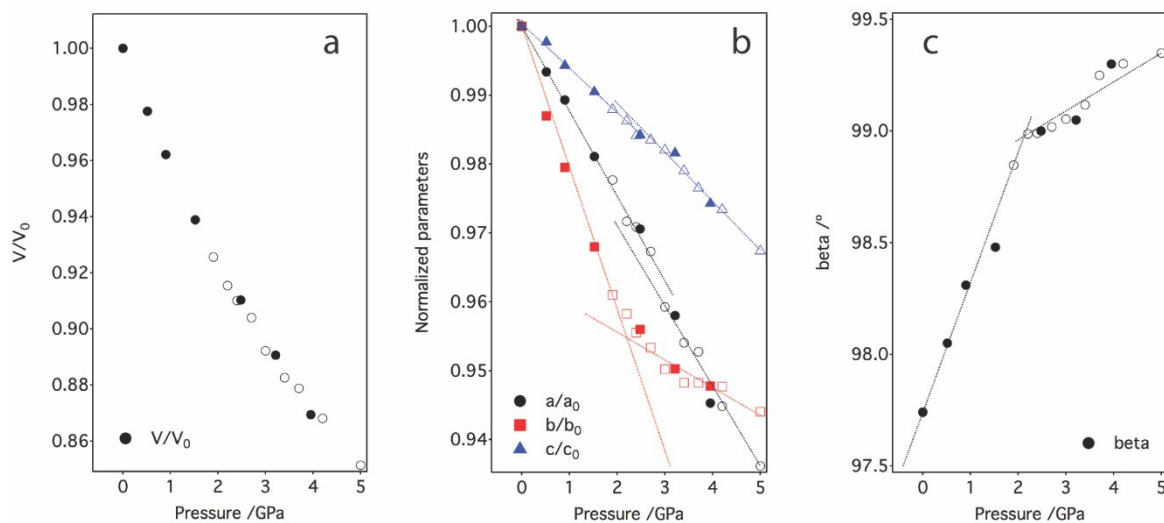
Table SI3. BM3 EoS parameters for single crystal Zn(GlyTyr)₂.

Parameters	Value
$V_0 / \text{\AA}^3$	1082.00(6)
K_0 / GPa	21.9(9)
K'	4.2(7)

The bulk modulus obtained for Zn(GlyTyr)₂ is typical for organometallic compounds (10-30 GPa)^{16,1} and we can associate this lower value to the deformability of the intermolecular interactions. The evolution of unit cell parameters is completely different

respect to the behavior of the volume when the pressure increase (Figure 3 in the text). In general, the curves show a slope change around 2.2GPa that in general, means a possible phase transition.

Figure SI15. Comparison of the variation of the volume, cell parameters and beta angle with pressure for the HP-SCXRD experiments performed in MeOH:EtOH:water (filled symbols) and the PXRD experiments performed in MeOH:water (empty symbols). Lines are only for eye guide. Changes in the PTM or the use of polycrystalline sample or single crystals do not seem to affect the evolution in the unit cell parameters that follow the same regime.



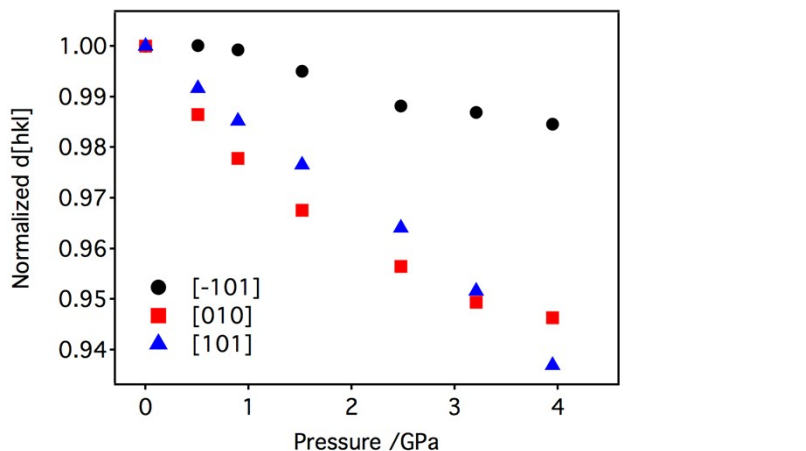
Variation of the cell parameters with pressure suggest that this compound presents an isostructural second-order phase transition. The space group does not change and the evolution of the volume cell does not show any discontinuity with the pressure increase in the range evaluated in this study.

Table SI4. Crystal data and HP structure refinement for $Zn(GlyTyr)_2$ between 0.51 and 3.95 GPa.

Pressure	0.51 GPa	0.90 GPa	1.52 GPa
Identification code	1588161	1588162	1588163
Empirical formula	$C_{22}H_{26}N_4O_8Zn$	$C_{22}H_{26}N_4O_8Zn$	$C_{22}H_{26}N_4O_8Zn$
M	539.84	539.84	539.84
Cryst. Syst.	Monoclinic	Monoclinic	Monoclinic
Space group	I2	I2	I2
a , Å	7.4416(6)	7.4106(6)	7.3494(5)
b , Å	5.4166(4)	5.3751(4)	5.3119(4)
c , Å	26.503(17)	26.411(17)	26.310(16)
α , °	90	90	90
β , °	98.046(18)	98.306(18)	98.483(17)
γ , °	90	90	90
V , Å³	1057.8(7)	1041.0(7)	1015.9(6)
Z	2	2	2
D_c /g cm⁻³	1.695	1.722	1.765
$F(000)$	560	560	560

$\mu(-\text{K}\alpha)$, mm ⁻¹	0.651	0.661	0.678
Reflections (collected/unique, (Rint))	675/571/0.029	651/570/0.024	564/512/0.018
Data/restrains/parameters	571/1/60	570/7/61	512/7/61
R1, wR [F ² >2σ(F ²)]	0.079/0.214	0.063/0.162	0.063/0.169
Goodness-of-fit on F ²	1.05	1.07	1.09
Largest diff. peak and hole (e Å ⁻³)	0.37/-0.41	0.29/-0.32	0.41/-0.31
Pressure	2.48 GPa	3.21 GPa	3.95 GPa
Identification code	1588164	1588165	1588166
Empirical formula	C ₂₂ H ₂₆ N ₄ O ₈ Zn	C ₂₂ H ₂₆ N ₄ O ₈ Zn	C ₂₂ H ₂₆ N ₄ O ₈ Zn
M	539.84	539.84	539.84
Cryst. Syst.	Monoclinic	Monoclinic	Monoclinic
Space group	I2	I2	I2
a, Å	7.2705(5)	7.1762(14)	7.0813(19)
b, Å	5.2464(4)	5.2148(8)	5.2012(10)
c, Å	26.144(18)	26.07(5)	25.88(10)
α, °	90	90	90
β, °	99.00(2)	99.05(6)	99.31(10)
γ, °	90	90	90
V, Å ³	985.0(7)	963.5(19)	941(4)
Z	2	2	2
D _v /g cm ⁻³	1.820	1.861	1.905
F(000)	560	560	560
$\mu(-\text{K}\alpha)$, mm ⁻¹	0.699	0.714	0.732
Reflections (collected/unique, (Rint))	539/477/0.016	465/435/0.016	387/367/0.020
Data/restrains/parameters	477/7/61	435/7/61	367/8/49
R1, wR [F ² >2σ(F ²)]	0.060/0.160	0.067/0.177	0.084/0.242
Goodness-of-fit on F ²	1.11	1.07	1.08
Largest diff. peak and hole (e Å ⁻³)	0.39/-0.32	0.27/-0.23	0.26/-0.21

Figure SI16. Comparison of the variation of the cell changes normalized to their value at ambient pressure for the crystallographic directions [-101], [010] and [101]. Overlaid structures of Zn(GlyTyr)₂ for each direction is shown in the next page.



[−101] [100] [010]

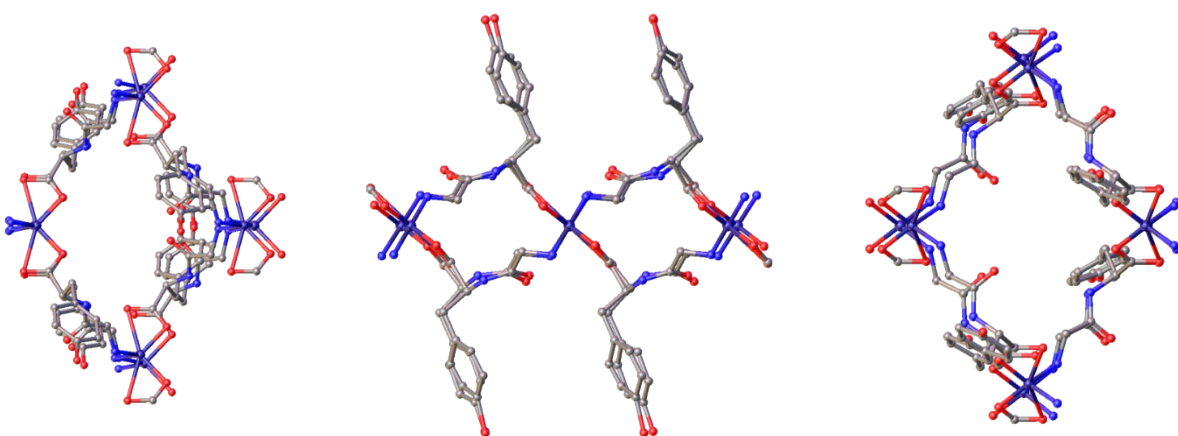


Figure SI17. Changes in the distance of the π-π interactions between 0-3.95 GPa defined as the distance between the centroid of neighbouring aromatic rings in the sidechain of Tyr.

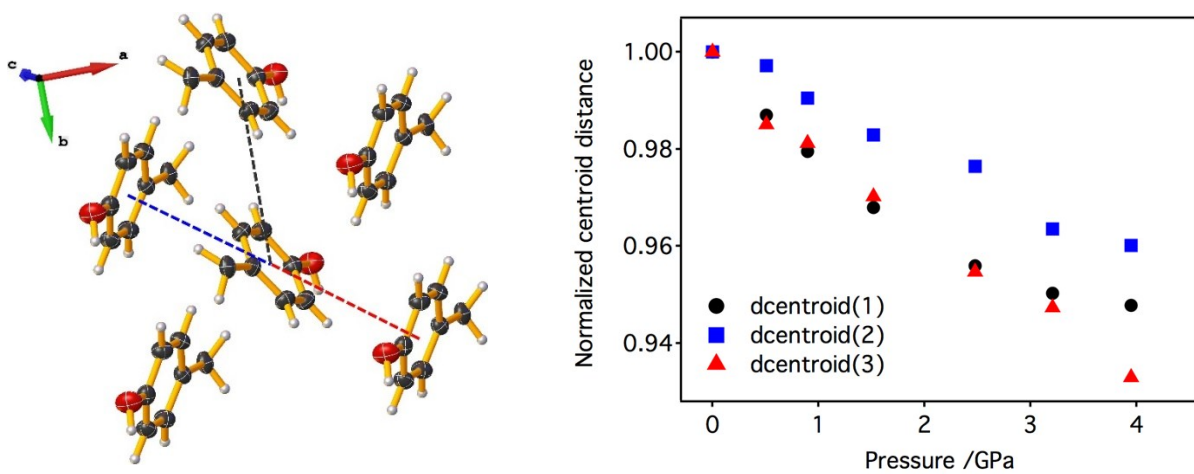


Table S15. Summary of the evolution of the parameters used for analysing the structural changes in Zn(GlyTyr)₂ at HP. For clarity, the figures included in the text represent the variation of volume and distances normalised to their respective values at ambient pressure by using the data below.

Evolution of the neighbouring Zn(II) sites across the MOF layer defined as diagonal 1 (d_1), diagonal 2 (d_2) and edge (Figure 4d):

Pressure /GPa	d_1 /Å	d_2 /Å	edge /Å
0.0001(1)	14.9816(4)	10.9754 (3)	9.2858(3)
0.51(4)	14.8832(14)	10.8332 (8)	9.2042(8)
0.90(4)	14.8212(14)	10.7502 (15)	9.1547(11)
1.52(4)	14.6988(12)	10.6238 (15)	9.0681(11)
2.48(4)	14.5410(13)	10.4928 (6)	8.9658(7)
3.21(4)	14.352(4)	10.4296 (1)	8.871(2)
3.95(4)	14.163(6)	10.4024(1)	8.786(2)

Conformational changes of the peptide defined as the torsion angles of the glycyl C-terminus (ψ) and threonine N-terminus (ϕ), that stand respectively for the dihedral angles (Figure 4e):

Pressure /GPa	ψ /° N2-C11-C10-N1	ϕ /° C2-C1-N1-C10
0.000(1)	164.1(3)	-109.4(3)
0.51(4)	159(3)	-109(4)
0.90(4)	164(3)	-111(3)
1.52(4)	160(3)	-108(4)
2.48(4)	157(3)	-101(4)
3.21(4)	154(4)	-102(5)
3.95(4)	146(6)	-91(8)

Hydrogen bond distances and angles (Figure 4f):

Pressure /GPa	D-H-A = N1-H1-O2(i)			
	d(D-H)/Å	d(H-A)/Å	d(D-A)/Å	D-H-A/°
0.000(1)	0.86	1.98	2.831(4)	169
0.51(4)	0.86	1.94	2.79(3)	168
0.90(4)	0.86	1.93	2.75(2)	158
1.52(4)	0.86	1.92	2.77(2)	173
2.48(4)	0.86	1.86	2.72(2)	177
3.21(4)	0.86	1.88	2.73(3)	170
3.95(4)	0.86	1.90	2.72(6)	160

(i) x,1+y,z

Pressure /GPa	D-H-A = O4-H4-O3(ii)			
	d(D-H)/Å	d(H-A)/Å	d(D-A)/Å	D-H-A/°

0.000(1)	0.82	1.89	2.643(4)	152
0.51(4)	0.82	1.88	2.64(4)	148
0.90(4)	0.82	2.09	2.54(3)	115
1.52(4)	0.82	2.00	2.54(4)	122
2.48(4)	0.82	2.10	2.56(4)	120
3.21(4)	0.82	2.05	2.47(4)	118
3.95(4)	0.82	1.99	2.50(9)	110

(ii) 3/2-x, 1/2+y, 3/2-z

Pressure /GPa	D-H-A = N2-H2B-O4(ii)			
	d(D-H)/Å	d(H-A)/Å	d(D-A)/Å	D-H-A/°
0.0001(1)	0.89	2.23		143
0.51(4)	0.89	2.16		144
0.90(4)	0.89	2.17		140
1.52(4)	0.89	2.17		139
2.48(4)	0.89	2.23		102
3.21(4)	0.90	1.96		138
3.95(4)	0.90	1.85		133

(ii) 3/2-x, 1/2+y, 3/2-z

Distances of the π-π interactions between the centroids of neighbouring aromatic rings (Figure SI15):

Pressure /GPa	Cg-Cg(i) /Å	Cg-Cg(ii) /Å	Cg-Cg(iii) /Å
0.0001(4)	5.488(4)	4.6125(4)	4.672(4)
0.51(4)	5.42(3)	4.60(3)	4.60(3)
0.90(4)	5.37(2)	4.57(2)	4.58(2)
1.52(4)	5.31(3)	4.52(2)	4.53(2)
2.48(4)	5.25(3)	4.51(2)	4.46(2)
3.21(4)	5.21(3)	4.45(3)	4.43(3)
3.95(4)	5.20(3)	4.43(3)	4.36(3)

(i)x, y-1, z (black); (ii)1/2-x,-1/2+y,3/2-z (blue); (iii)3/2-x,1/2+y,3/2-z (red)

SI6. References

- [1] Rigaku Oxford Diffraction, **2017**, *CrysAlisPro Software system, version 1.171.38.46*, Rigaku Corporation, Oxford, UK
- [2] Sheldrick, G. M. *Acta Cryst.* **2015**, A71, 3-8.
- [3] Sheldrick, G. M. *Acta Cryst.* **2008**, A64, 112-122.
- [4] Spek, A. L. *Acta Cryst.* **2009**, D65, 148-155.
- [5] J. Rabone, Y. F. Ye, S. Y. Chong, K. C. Stylianou, J. Bacsa, D. Bradshaw, G. R. Darling, N. G. Berry, Y. Z. Khimyak, A. Y. Ganin, P. Wiper, J. B. Claridge, M. J. Rosseinsky, *Science* **2010**, 329, 1053.
- [6] C. Martí-Gastaldo, D. Antypov, J. E. Warren, M. E. Briggs, P. A. Chater, P. V. Wiper, G. J. Miller, Y. Z. Khimyak, G. R. Darling, N. G. Berry, M. J. Rosseinsky, *Nat. Chem.* **2014**, 6, 343.
- [7] C. Martí-Gastaldo, J. E. Warren, K. C. Stylianou, N. L. O. Flack, M. J. Rosseinsky, *Angew. Chem. Int. Ed.* **2012**, 51, 11044.
- [8] Mao, H. K.; Xu, J.; Bell, P. M. *J. Geophys. Res.* **1986**, 91, 4673.
- [9] Errandonea, D. *Cryst. Res. Technol.* **2015**, 50, 729.
- [10] Fauth, F.; Peral, I.; Popescu, C.; Knapp, M. *Synchrotron Powder Diffr.* **2013**, 28, S360.
- [11] Hammersley, A. P.; Svensson, S. O.; Hanfland, M.; Fitch, A. N.; Häusermann, D. *High Press. Res.* **1996**, 14, 235.
- [12] Larson, A. C.; von Dreele, R. B. GSAS: General Structure Analysis System. *Los Alamos National Laboratory Report* **2000**, 86-748.
- [13] Angel, R. J.; Bujak, M.; Zhao, J.; Gatta, G.D.; Jacobsen, S. D. *J. Appl. Crystallogr.* **2007**, 40, 26-32.
- [14] Klotz, S.; Chervin, J.; Munsch, P.; Le Marchand, G. *J. Phys. D. Appl. Phys.* **2009**, 42, 75413, 2009.
- [15] Errandonea, D.; Muñoz, A.; Gonzalez-Platas, J. *J. Appl. Phys.* **2014**, 115, 216101:1-3